Thermal equilibration near the critical point: Effects due to three dimensions and gravity

Robert F. Berg
Thermophysics Division, Chemical Science and Technology Laboratory, Technology Administration, U.S. Department of Commerce, National Institute of Standards and Technology, Gaithersburg, Maryland 20899
(Received 15 March 1993)

Two calculations are presented that clarify how the density profile equilibrates near the liquid-vapor critical point. Both use the equation of heat transfer recently improved to account for the large compressibility near the critical point. Previous work by others indicated that in one dimension the slowest mode of this equation relaxes at a rate four times faster than that predicted by the older, usual equation of heat transfer. However, this is not always true in higher dimensions. The first calculation demonstrates this for the cases of isobaric modes excited by temperature gradients in a rectangle and in a thin disk. For thin experimental cells with isothermal walls the slowest mode is accurately estimated by the usual heat-transfer equation. The second calculation indicates that gravity-induced stratification plays an insignificant role in determining the final relaxation rate. This is done by estimating the size of the $\mathbf{v}\cdot\nabla P$ term in the improved heat-transfer equation.

PACS number(s): 66.10.Cb, 64.60.−i, 65.70.+y, 05.70.Jk

I. INTRODUCTION

The thermal diffusivity D_T vanishes near the liquid-vapor critical point. Until recently this fact plus the usual equation of heat transfer

$$\dot{T}=D_T\nabla^2 T \tag{1}$$

were seen by most workers as the complete picture for the very slow relaxation times often observed in one-phase critical point experiments. In the one-phase region, these times are of the order of

$$T\sim\frac{L^2}{D_T}\ , \tag{2}$$

where L is a characteristic length of the fluid's container. However, in 1984, Straub and co-workers [1] measured very short temperature equilibration times close to the critical point even when low gravity was used to suppress convection. This and related puzzles led to the realization [2–5] that the divergence of the fluid's compressibility near its critical point significantly affects thermal equilibration.

Calculations accounting for the diverging compressibility led to the replacement of Eq. (1) by an improved heat-transfer equation

$$\dot{T}-\left[1-\frac{c_V}{c_P}\right]\left[\frac{\partial T}{\partial P}\right]_\rho \dot{P}=(\rho c_P)^{-1}\nabla(\lambda\nabla T)\ , \tag{3}$$

where T, P, ρ, and λ are the temperature, pressure, density, and thermal conductivity, and c_P and c_V are the heat capacities per unit mass at constant pressure and volume. Examinations of the time dependence of Eq. (3) in one dimension gave two interesting predictions about the fluid temperature following a perturbation. First, for isothermal boundaries, the initial temperature relaxation was nonexponential and fast, typically lasting a few seconds instead of the tens of minutes or even hours predicted by Eq. (1) for typical experimental conditions. Second, the final exponential relaxation was predicted to be 4 times faster than that predicted by Eq. (1) [2]. In the only quantitative test so far published, Behringer, Onuki, and Meyer [6] reanalyzed previous measurements in thermal conductivity cells [7,8] and found relaxation rates only slightly lower than this latter prediction.

The improved heat-transfer equation is necessary though perhaps not sufficient for explaining the results of equilibration experiments carried out in Earth's gravity. For example, in 1965, Straub [9] measured the relaxation of the vertical density profile of NO_2 following an expansion and compression cycle and found that complete relaxation could take more than 1 day. Since then, similar observations have been made by others (for example, see Refs. [10–12]). During these long equilibration times, deviations of the vertical density profile from its final form are coupled to vertical temperature gradients through the equation of state. However, there remains uncertainty about the role of gravity in the equilibration process.

These results concerning relaxation rates near liquid-vapor critical points are of particular interest for the design of practical critical point experiments where time is limited, for example those carried out on sounding rocket or Space Shuttle flights. Because equilibration times can be long enough to constrain experiments of even 1 week's duration, the factor of 4 difference between the predictions of Eqs. (2) and (3) is potentially important. Furthermore, gravity's influence on the equilibration processes must be understood sufficiently well to predict low-gravity equilibration times from measurements of equilibration on Earth.

This paper presents two calculations which clarify how the density profile equilibrates near the critical point. The first calculation uses simple examples to demonstrate that the factor of 4 in the final relaxation, calculated by

Onuki, Hao, and Ferrell [2] and generalized to finite c_P/c_V by Behringer, Onuki, and Meyer [6], occurs only in systems which are effectively one-dimensional (1D). The key idea is that, in addition to the nonisobaric solutions excited by changes in the average temperature, there can also be isobaric solutions excited by temperature gradients. In the limit of a narrow geometry, the isobaric solution decays as slowly as the solution of the usual heat-transfer equation.

The second calculation indicates that gravity is not important in determining the final relaxation rate of the density profile, provided that the equilibrium density profile near the critical point is approximately linear.

This paper is organized as follows: Sections II and III briefly review the improved heat-transfer equation, Eq. (3), and its solutions in one dimension. Sections IV and V use a 2D rectangle and a 3D disk to illustrate the qualitative differences of isobaric relaxation in higher dimensions. Section VI estimates the effect of gravity on the final exponential relaxation rate, and Sec. VII concludes.

II. THE IMPROVED HEAT-TRANSFER EQUATION

Ferrell and Onuki [13] first described the theory for the qualitatively different thermal relaxation which occurs near the critical point. Appendix A reviews a simpler derivation, first published by Boukari *et al.* [3], of the improved heat-transfer equation. Starting from Landau and Lifshitz's [14] general equation for the transport of the fluid entropy s,

$$\rho T(\dot{s}+\nabla s\cdot\mathbf{v})=\nabla\cdot(\lambda\nabla T)\ , \tag{4}$$

Boukari *et al.* ignored the fluid's velocity $\mathbf{v}$ and obtained the linearized form

$$\dot{T}-\left[1-\frac{c_V}{c_P}\right]\left[\frac{1}{V}\right]\int \dot{T}\,dV=D_T\nabla^2 T\ , \tag{5}$$

where the thermal diffusivity is defined by

$$D_T\equiv\frac{\lambda}{\rho c_P}\ . \tag{6}$$

In comparison with the usual heat-transfer equation, Eq. (1), the improved heat-transfer equation, Eqs. (3) and (5), contains an additional term proportional to $\dot{P}$ which cannot be ignored near the critical point. This global term causes the "critical speeding up" of the initial temperature equilibration. Although for a closed cell with an isothermal boundary the final, exponential part of the temperature equilibration is very small, of order c_V/c_P, the sensitive dependence of density on temperature causes an observable effect on the density distribution. Under certain conditions, the slowest mode of Eq. (5) is characterized by a time constant which is 4 times faster than predicted by Eq. (1).

There can be, however, solutions of Eq. (3) for which $\dot{P}=0$. Such isobaric solutions represent modes excited by temperature gradients, and they are also solutions of the more usual equation (1). They are important because, except in one dimension, the slowest time constant for geometries of narrow aspect ratio is very nearly the same as that calculated by Eq. (1). This will be shown in Secs. III–V.

III. SOLUTION IN ONE DIMENSION

Consider the relaxation to equilibrium following a temperature disturbance in a one-dimensional cell of length $2x_0$ with isothermal boundary conditions, namely,

$$\delta T(\pm x_0,t)\equiv 0\ , \tag{7}$$

where the temperature deviation δT is defined by

$$\delta T(x,t)\equiv T(x,t)-T(\pm x_0)\ . \tag{8}$$

After a time long compared to x_0^2/D_T, the solutions to Eq. (5) are purely exponential in time. In this limit and in the limit where the heat-capacity ratio c_P/c_V is much greater than 1 (true near the critical point), the slowest modes are the nonisobaric mode [5,6],

$$\delta T(x,t)=T_0[1+\cos(qx)]e^{-t/\tau}\ , \tag{9}$$

and the isobaric mode,

$$\delta T(x,t)=T_0\sin(qx)e^{-t/\tau}\ . \tag{10}$$

For both of these modes, pictured in Fig. 1, the wave vector q is given by

$$qx_0=\pi\ , \tag{11}$$

and the relaxation time constant τ is

$$\tau=\frac{1}{D_T q^2}=\frac{x_0^2}{\pi^2 D_T}\ . \tag{12}$$

As first pointed out by Onuki, Hao, and Ferrell [2], this relaxation time is 4 times faster than the slowest mode of the usual equation (1).

IV. SOLUTION IN A RECTANGLE

To illustrate the importance of an extra spatial dimension consider the case of a rectangle of width $2x_0$ and height $2y_0$. For isothermal boundary conditions, namely,

$$\delta T(\pm x_0,y,t)=\delta T(x,\pm y_0,t)\equiv 0\ , \tag{13}$$

Eq. (5) does not have a simple nonisobaric solution. However, the solution for the slowest isobaric mode is

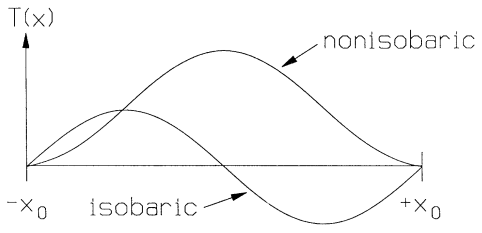

FIG. 1. The slowest relaxation modes of Eq. (5) in a one-dimensional cell of length $2x_0$. The isobaric and nonisobaric modes have the same time constant, which is 4 times faster than the corresponding modes of the usual equation (1).

simply

$$\delta T(x,y,t)=T_0\cos(qx)\sin(ky)e^{-t/\tau}\ , \tag{14}$$

as depicted by Fig. 2. In Eq. (14), the wave vectors are given by

$$qx_0=\frac{\pi}{2}\quad\text{and}\quad ky_0=\pi\ , \tag{15}$$

and the time constant is

$$\tau=\frac{1}{(q^2+k^2)D_T}=\left[\frac{\pi^2}{4x_0^2}+\frac{\pi^2}{y_0^2}\right]^{-1}D_T^{-1}\ . \tag{16}$$

For the case of a narrow rectangle, where $x_0 \ll y_0$, the time constant becomes

$$\tau\cong\frac{4x_0^2}{\pi^2 D_T}[1-4(x_0/y_0)^2]\ , \tag{17}$$

almost 4 times slower than the corresponding one-dimensional time constant, Eq. (12), and only slightly faster than the slowest mode of the usual heat-transfer equation, Eq. (1), where

$$\tau\cong\frac{4x_0^2}{\pi^2 D_T}[1-(x_0/y_0)^2]\ . \tag{18}$$

Hao [15] has recently estimated the behavior of nonisobaric relaxation in a narrow rectangle with an isothermal boundary and found that, as shown above for isobaric relaxation, the final relaxation also has a time constant close to that given by Eq. (1). Unlike the isobaric case, this behavior is predicted to occur only after the very long time y_0^2/D_T, and thus its amplitude may be too small to be observable. In the intermediate regime $x_0^2/D_T < t \ll y_0^2/D_T$ the relaxation is similar to the one-dimensional case [Eq. (12)] with corrections of order x_0/y_0.

In summary, in the limit of a narrow rectangle, the time constant for the slowest modes is 4 times slower than in one dimension. Although the nonisobaric mode's final relaxation in a thin experimental cell may be unobservable, the isobaric mode's final relaxation in a simple geometry is easily calculated and should be purely exponential at times much greater than x_0^2/D_T.

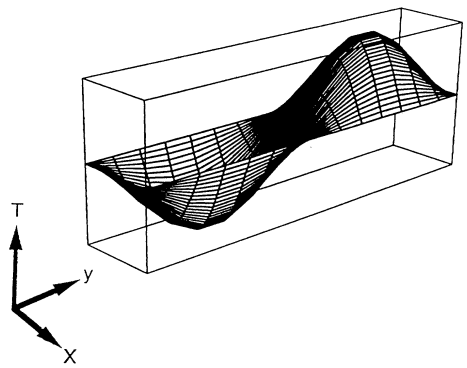

FIG. 2. Temperature distribution map showing relaxation of the slowest isobaric mode in a rectangle with isothermal boundaries, Eq. (14).

V. SOLUTION IN A 3D DISK

Many experiments near liquid-vapor critical points have been carried out in thin, disk-shaped ("pancake") cells. Suppose one has such a container of radius R and height $2z_0$ with isothermal boundaries:

$$\delta T(R,\phi,z,t)=\delta T(r,\phi,\pm z_0,t)\equiv 0\ , \tag{19}$$

where polar coordinates (r,ϕ,z) are used [see Fig. 3(a)]. As was the case for the narrow rectangle, when one uses Eq. (5) for a thin disk containing a fluid near its critical point, the longest isobaric time constant is much closer to the conventional time constant predicted by Eq. (1) than the one-dimensional prediction.

In the limit of a thin disk ($z_0 \ll R$) there is a family of slowest isobaric modes given by

$$\delta T(r,\phi,z,t)=\sum_{a=1}^{\infty}\sum_{b=1}^{\infty}T_{ab}\cos(qz)J_a(k_{ab}r)\times\cos(a\phi)e^{-t/\tau_{ab}}\ . \tag{20}$$

Because the faster decaying solutions proportional to $\sin(nqz)$ and to $\cos(nqz)$, $n>1$, are not included here, the members of this family differ only in the form of their lateral (r,ϕ) temperature variation. [For simplicity, solutions proportional to $\sin(a\phi)$ are also dropped.] The wave vectors q and k_{ab} are determined by the isothermal boundary conditions:

$$qz_0=\frac{\pi}{2} \tag{21}$$

and

$$J_a(k_{ab}R)=0\ , \tag{22}$$

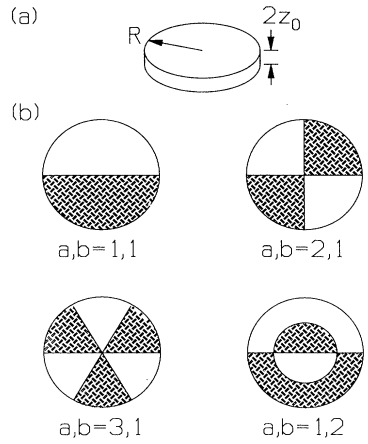

FIG. 3. In a thin disk-shaped cell, the slowest time constants for relaxation of gradients are nearly independent of the lateral variations in temperature. For a disk with a diameter-to-thickness ratio of 10, the four slowest modes have time constants equal to within ±7%. (a) Sketch of a "pancake" cell. (b) Nodal maps of the four slowest modes. Ordered from slowest to fastest they correspond to the zeros j_{11}, j_{21}, j_{31}, and j_{12}.

yielding the time constant for mode ab of

$$\tau_{ab}=\frac{1}{[q^2+k_{ab}^2+(a/R)^2]D_T}=\left[\frac{\pi^2}{4z_0^2}+\frac{j_{ab}^2+a^2}{R^2}\right]^{-1}D_T^{-1}, \tag{23}$$

where j_{ab} denotes the bth zero of the Bessel function J_a.

In the limit of the thin disk, Eq. (23) becomes

$$\tau_{ab}\cong\left[\frac{4z_0^2}{\pi^2 D_T}\right]\left[1-\frac{4(j_{ab}^2+a^2)}{\pi^2}\left[\frac{z_0}{R}\right]^2\right]. \tag{24}$$

To illustrate the close spacing of these slowest time constants, for a thin disk with aspect ratio $R/z_0=10$, the relative sizes of the correction term in Eq. (24) for the slowest four modes, illustrated in Fig. 3(b), are only

$$\frac{4(j_{ab}^2+a^2)}{\pi^2}\left[\frac{z_0}{R}\right]^2=6.4\%,\ 12.3\%,\ 20.1\%,\ \text{and}\ 20.4\%\ . \tag{25}$$

In comparison, the usual equation for noncritical heat transfer, Eq. (1), predicts a slowest relaxation time of

$$\tau\cong\left[\frac{4z_0^2}{\pi^2 D_T}\right]\left[1-\frac{4j_{01}^2}{\pi^2}\left[\frac{z_0}{R}\right]^2\right], \tag{26}$$

which is slower than the slowest time constant, τ_{11} of Eq. (24), by only $6.36\%-2.34\%=4.02\%$.

Note that for the other limiting aspect ratio, namely, the case of a long, thin cylinder, where $R\ll z_0$, the slowest isobaric mode has the time constant

$$\tau\cong\left[\frac{R^2}{j_{01}^2 D_T}\right]\left[1-\left[\frac{\pi}{j_{01}}\right]^2\left[\frac{R}{z_0}\right]^2\right], \tag{27}$$

again only slightly faster than the prediction of Eq. (1).

VI. GRAVITY'S EFFECT ON THE FINAL RELAXATION

Gravity is certainly important near the critical point because it causes equilibrium vertical density differences of several percent in typical liquid-vapor experiments [16]. This section will examine gravity's effect on the evolution of a linear density profile following a small change in the fluid container's wall temperature. Using Eq. (4) as a starting point it will be shown that, through the fluid's downward velocity, the effect of gravity is of first order in the temperature perturbation δT and is thus potentially important. However, the size of the relevant term turns out to be too small to significantly change the final relaxation time constant.

Gravity can be incorporated into Eq. (4), the original equation of motion for the entropy s, by retaining the velocity v. Using the relations in Sec. II together with the relation

$$\nabla s=\left[\frac{\partial s}{\partial T}\right]_P\nabla T+\left[\frac{\partial s}{\partial P}\right]_T\nabla P\ , \tag{28}$$

Eq. (4) can be written as

$$\dot{T}+\nabla T\cdot\mathbf{v}-\left[1-\frac{c_V}{c_P}\right]\left[\frac{\partial T}{\partial P}\right]_\rho(\dot{P}+\nabla P\cdot\mathbf{v})=(\rho c_P)^{-1}\nabla(\lambda\nabla T)\ . \tag{29}$$

(In what follows, only the vertical components of the velocity and pressure gradient are considered, hence the vector notation will be dropped.)

In contrast to Eq. (3), Eq. (29) has terms proportional to $\nabla T\cdot v$ and $\nabla P\cdot v$ on the left-hand side. Here I will consider the relative importance of these two extra terms in the limit of long times after a small disturbance, namely, the final exponential decay of the temperature deviation δT where the velocity v and the amplitudes δT and δP are all very small.

The $\nabla T\cdot v$ term is the product of two small perturbations and thus becomes negligible in comparison with the first term.

In contrast, the $\nabla P\cdot v$ term cannot be ignored because, in Earth's gravity g, it can be first order in the amplitude δT. This is because, for a fluid in hydrostatic equilibrium, the pressure gradient in the vertical direction is

$$\nabla P=\frac{dP}{dz}=-g\rho \tag{30}$$

and does not become small with time.

The size of the $\nabla P\cdot v$ term of Eq. (29) can be estimated by analyzing the following gedanken experiment: Consider the tall, narrow experimental cell in Fig. 4 having perfectly conducting side walls at $\pm x_0$ and insulating walls at $\pm y_0$ and at $\pm z_0$, with $y_0, z_0 \gg x_0$. Its interior is filled with a fluid whose average density is the critical density ρ_c and whose temperature is initially held close above the critical temperature T_c. Gravity and the fluid's

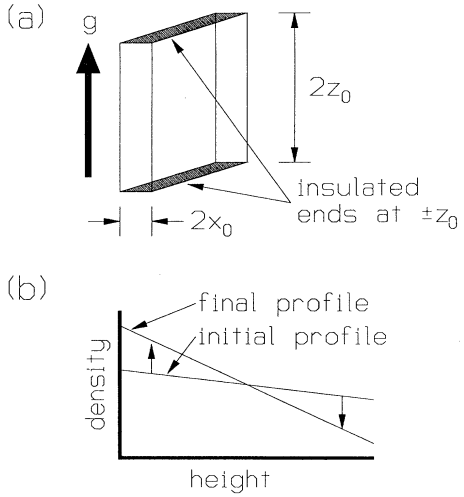

FIG. 4. The model for estimating the effect of gravity on the final equilibration time constant. The cell's wall temperature steps down from $(1+\epsilon)T_c+\Delta T$ to $(1+\epsilon)T_c$, and the slope of the density profile $\rho(z)$ increases. (a) The cell's boundary conditions. (b) The initial and final density profiles.

compressibility cause the density to stratify into an equilibrium profile $\rho(z)$. Now, starting at $(1+\epsilon)T_c+\Delta T$ at time $t=0$, quickly cool the wall temperature by the small amount $\Delta T \ll \epsilon T_c$. [Here, $\epsilon \equiv (T-T_c)/T_c$ is the reduced temperature.] The final result will be a steeper gradient in the z direction of the equilibrium density profile:

$$\rho(z,(1+\epsilon)T_c+\Delta T) \rightarrow \rho(z,(1+\epsilon)T_c) \ . \tag{31}$$

During the initial "critical speeding up" period the fluid's density increases near the walls and decreases in the interior, rapidly cooling the interior to slightly above the wall temperature. Afterwards, in addition to the net motion of the fluid from the top half of the cell toward the bottom half, the approach to the final equilibrium necessarily requires horizontal motion of the fluid from near the cell's walls toward the cooling interior. However, to a very good approximation, the pressure depends only on the height z. Thus $\nabla P \cdot v$ can be estimated from the average downward motion of the fluid while ignoring the horizontal component of v.

Two additional assumptions are made concerning the density profile. First, that it is linear in z (applicable in most experiments at reduced temperatures $\epsilon > 3\times 10^{-4}$) and second, that it relaxes exponentially with a time constant τ according to

$$\rho(z,t)=\rho_c-\rho_1\left[\frac{z}{H_0}\right][1-\alpha e^{-t/\tau}] \ . \tag{32}$$

Here the final density profile is characterized by the parameters ρ_1 and the gravitational scale height [16]

$$H_0 \equiv \frac{P_c}{g\rho_c} \ , \tag{33}$$

where P_c is the critical pressure. The small parameter α measures the difference between the initial and final density profiles.

The flow at height z is equal to the total mass change above z, giving

$$\rho(z,t)v(z,t)=\int_z^{z_0}\dot{\rho}(z',t)dz' \ . \tag{34}$$

Putting the density profile equation (32) into Eq. (34) and ignoring small terms, one obtains an estimate for the vertical velocity field $v(z,t)$:

$$\rho_c v(z,t) \cong -\left[\frac{\alpha\rho_1}{2\tau H_0}\right](z_0^2-z^2)e^{-t/\tau} \ . \tag{35}$$

The pressure-gradient term is thus largest at the middle, $z=0$, where it has the value

$$-\left[\frac{\partial T}{\partial P}\right]_\rho \nabla P\cdot v \cong \left[\frac{\partial T}{\partial P}\right]_\rho g\rho_c v(0,t) \cong -\left[\frac{\partial T}{\partial P}\right]_\rho \frac{\alpha g\rho_1 z_0^2}{2\tau H_0}e^{-t/\tau} \ . \tag{36}$$

Final evaluation of the pressure-gradient term requires estimating the factor $\alpha\rho_1$ from the difference of the initial and final density profiles in Eq. (32). In the restricted cubic model [16] and at reduced temperatures where the correlation length is only a weak function of height z, the density profile is nearly proportional to z, allowing one to write the profile difference as

$$\left[\frac{z}{H_0}\right]\alpha\rho_1 \le z\Delta T\frac{\partial}{\partial T}\left[\frac{\partial\rho}{\partial z}\right] \tag{37}$$

$$= z\Delta T\frac{\partial}{\partial T}\left[-\left[\frac{\rho_c}{H_0}\right]\Gamma\epsilon^{-\gamma}\right] \tag{38}$$

$$= \gamma\Gamma\rho_c\left[\frac{z}{H_0}\right]\left[\frac{\Delta T}{T_c}\right]\epsilon^{-(\gamma+1)} \ , \tag{39}$$

where $\gamma=1.24$ and Γ are, respectively, the critical exponent and amplitude for the normalized susceptibility. Note that

$$\alpha \le \gamma\left[\frac{\Delta T}{\epsilon T_c}\right] \ll 1 \ , \tag{40}$$

which is consistent with the assumption of a small density change in Eq. (32). Inserting Eq. (39) into Eq. (36) gives an expression for the pressure-gradient term in terms of known quantities:

$$\left[\frac{\partial T}{\partial P}\right]_\rho \nabla P\cdot v \cong \frac{\gamma\Gamma}{2}\epsilon^{-(\gamma+1)}\left[\frac{T_c}{P_c}\frac{\partial P}{\partial T}\right]_\rho^{-1} \times \left[\frac{z_0}{H_0}\right]^2\frac{\Delta T}{\tau}e^{-t/\tau} \ . \tag{41}$$

Now the pressure-gradient term in the heat-transfer equation, Eq. (29), can be compared against the first-order term in the absence of gravity, which is [2,5]

$$\dot{T}=-\delta T\frac{1}{\tau}e^{-t/\tau} \approx \frac{-2\Delta T}{c_P/c_V}\frac{1}{\tau}e^{-t/\tau} \ . \tag{42}$$

The ratio of the pressure-gradient term to the $\dot{T}$ term is thus

$$-\left[\frac{\partial T}{\partial P}\right]_\rho \frac{\nabla P\cdot v}{\dot{T}} \approx \frac{\gamma\Gamma}{2}(c_P/c_V)_0\left[\frac{T_c}{P_c}\frac{\partial P}{\partial T}\right]_\rho^{-1} \times \left[\frac{z_0}{H_0}\right]^2\epsilon^{-(2\gamma+1)} \ , \tag{43}$$

where the estimate of $c_P/c_V=(c_P/c_V)_0\epsilon^{-\gamma}$ is derived in Appendix B.

For a typical cell height of $2z_0=10$ mm, the smallest reduced temperature ϵ where the density profile is roughly linear is $\epsilon \approx 3\times 10^{-4}$. Using SF_6 at this reduced temperature as an example, the relative importance of the pressure-gradient term is

$$-\left[\frac{\partial T}{\partial P}\right]_\rho \frac{\nabla P\cdot v}{\dot{T}} \approx \frac{(1.24)(0.046)(0.013)(1.0\times 10^{-5})^2}{(4)(6)}\epsilon^{-3.48}$$

$$= 0.006 \ll 1 \ .$$

Thus, at reduced temperatures where the density profile is approximately linear, the $\nabla P \cdot v$ term can be ignored, and the final equilibration time constant is nearly the same in the presence of gravity-induced stratification as it would be in the absence of stratification.

VII. CONCLUSIONS

The late stage of one-phase equilibration near the critical point can be defined as the times when the fluid's temperature distribution can be described by the sum of independent spatial modes, each decaying exponentially in time. In one dimension, the slowest mode decays 4 times faster than predicted by the usual heat-transfer equation, Eq. (1). However, this is not true for real containers with isothermal walls, and for thin cells the slowest isobaric mode of Eq. (5) decays almost as slowly as the slowest mode of the conventional equation (1).

For cells having other than isothermal boundaries, the slowest isobaric mode may not be significantly slower than the slowest nonisobaric mode. This was the case for the thermal conductivity cells analyzed by Behringer, Onuki, and Meyer [6], where the derivative of temperature with height, and not the temperature, was specified at the top of the cell. Even in cells with isothermal walls, the excited amplitude of the slowest isobaric mode will depend on asymmetries such as heater locations and, in Earth's gravity, the cell's orientation.

In experimental situations where temperature or density gradients are deliberately imposed across the diameter of a thin disk-shaped cell [10,11] it is useful to realize that Eq. (24) implies that the slowest modes have relaxation time constants which are closely spaced. Lateral temperature deviations created by time-dependent temperature gradients, along with their associated density deviations, can thus be approximately described by a sum of independent spatial modes all relaxing with the same time constant.

At reduced temperatures where the density profile does not cause significant height dependence of the fluid properties, gravity should have a very limited effect on the time constant for the equilibration of the density profile near the critical point. This is because the $\nabla P \cdot v$ term is small compared to the $\dot{T}$ term in Eq. (29). At reduced temperatures closer to T_c, where the equilibrium density profile is strongly nonlinear, the assumptions of Sec. VI do not hold. Nevertheless, assuming the $\Delta P \cdot v$ term remains small, gravity's only effect on the relaxation will be through the height dependence of the fluid's properties.

The above results are useful for understanding experiments where the vertical density profile relaxation is observed following a change in the sample cell's wall temperature [9–12]. First, gravity can be neglected in the calculation of the time constant for relaxation at temperatures where the density profile is approximately linear. Second, the temperature field created within the fluid can be seen as the sum of two effects. The first effect is the nonisobaric relaxation due to the change in the fluid's average temperature. The second effect is the isobaric mode associated with the vertical temperature gradient necessary to support the nonequilibrium vertical density profile. If the cell is tall (height $2z_0$) and narrow (width $2x_0$), the amplitude of the final relaxation of the nonisobaric mode occurring at very long times ($t > z_0^2/D_T$) will be negligible. In the intermediate regime $x_0^2/D_T < t < z_0^2/D_T$, where density deviations are observable, the isobaric mode will be slower than the first effect by about a factor of 4, and it will govern the final relaxation rate of the vertical density profile.

ACKNOWLEDGMENTS

This work was stimulated by the observations of density relaxation in the Thermal Equilibration Experiment, headed by Allen Wilkinson of NASA Lewis Research Center and which made use of the European Space Agency's Critical Point Facility. I am especially grateful for the 1g quantitative measurements made by Ludwig Eicher and Johannes Straub. I acknowledge useful conversations with Hacene Boukari, Jack Douglas, Robert Gammon, Johannes Straub, and particularly Hong Hao, Horst Meyer, and Michael Moldover. This work was supported in part by NASA under Contract No. C-32009-M.

APPENDIX A: DERIVATION OF THE IMPROVED HEAT-TRANSFER EQUATION

The improved heat-transfer equation, Eq. (3), can be derived [3] from Landau and Lifshitz's [14] general equation for the transport of the fluid entropy s, Eq. (4), by ignoring the velocity term. Using the relations

$$\dot{s} = \left[\frac{\partial s}{\partial T}\right]_P \dot{T} + \left[\frac{\partial s}{\partial P}\right]_T \dot{P} , \tag{A1}$$

$$\rho T \left[\frac{\partial s}{\partial T}\right]_P \equiv \rho c_P , \tag{A2}$$

and

$$\rho T \left[\frac{\partial s}{\partial P}\right]_T = \left[\frac{T}{\rho}\right]\left[\frac{\partial \rho}{\partial T}\right]_P , \tag{A3}$$

Eq. (4) can be written as

$$\rho c_P \dot{T} + \left[\frac{T}{\rho}\right]\left[\frac{\partial \rho}{\partial T}\right]_P \dot{P} = \nabla \cdot (\lambda \nabla T) . \tag{A4}$$

Then, using the relation

$$c_P - c_V = -T\rho^{-2}\left[\frac{\partial P}{\partial T}\right]_\rho \left[\frac{\partial \rho}{\partial T}\right]_P \tag{A5}$$

in Eq. (A4) and dividing by ρc_P, one then gets the improved heat-transfer equation, Eq. (3).

In order to express Eq. (3) in terms of only the temperature, one writes

$$\dot{\rho} = \left[\frac{\partial \rho}{\partial T}\right]_P \dot{T} + \left[\frac{\partial \rho}{\partial P}\right]_T \dot{P} . \tag{A6}$$

In a closed cell, the spatial integral over the volume V gives zero on the left-hand side. In the absence of gravi-

ty, ∇P is almost exactly zero, so that the pressure changes uniformly throughout the cell. Thus, for temperature changes small compared to $(T-T_c)$, Eq. (A6) yields an expression for $\dot{P}$ in terms of the spatial integral of $\dot{T}$:

$$\dot{P}=-\left[\frac{\partial\rho}{\partial T}\right]_P\left[\frac{\partial P}{\partial\rho}\right]_T\frac{1}{V}\int\dot{T}\,dx\ . \tag{A7}$$

Inserting Eq. (A7) into Eq. (3) then gives Eq. (5).

APPENDIX B: HEAT-CAPACITY RATIO γ_c

From Eq. (A5) the difference of the isobaric and isochoric heat capacities can be written in terms of the nondivergent slope $\partial P/\partial T$ and the reduced susceptibility χ_T^* as

$$c_P-c_V=-\left[\frac{T}{P}\frac{\partial P}{\partial T}\right]_\rho\left[\frac{T}{\rho}\frac{\partial\rho}{\partial T}\right]_P\left[\frac{P}{T\rho}\right] \tag{B1}$$

$$=\left[\frac{T}{P}\frac{\partial P}{\partial T}\right]_\rho^2\chi_T^*\left[\frac{P}{T\rho}\right]\ . \tag{B2}$$

Then the heat-capacity ratio can be estimated as

$$\frac{c_P}{c_V}\cong\frac{c_P-c_V}{c_V}=\left[\frac{T_c}{P_c}\frac{\partial P}{\partial T}\right]_{\rho_c}^2 Z_c\left[\frac{R}{Ac_V}\right]\chi_T^*\ , \tag{B3}$$

where R and A are the gas constant and molar weight and, for SF_6 [17],

$$Z_c\equiv\frac{P_c}{\rho_c}\frac{A}{T_cR}=0.284\ . \tag{B4}$$

The heat-capacity ratio near the critical point of SF_6 is thus

$$\frac{c_P}{c_V}\cong(6)^2(0.284)(0.028)(0.046\epsilon^{-\gamma})$$

$$\equiv(c_P/c_V)_0\epsilon^{-\gamma}=0.013\epsilon^{-\gamma}\ . \tag{B5}$$

[1] K. Nitsche, J. Straub, and R. Lange (unpublished); J. Straub and K. Nitsche, Fluid Phase Equil. **88**, 183 (1993).

[2] A. Onuki, H. Hao, and R. A. Ferrell, Phys. Rev. A **41**, 2256 (1990).

[3] H. Boukari, J. N. Shaumeyer, M. E. Briggs, and R. W. Gammon, Phys. Rev. A **41**, 2260 (1990).

[4] B. Zappoli, D. Bailly, Y. Garrobos, B. Le Neindre, P. Guenon, and D. Beysens, Phys. Rev. A **41**, 2264 (1990).

[5] A. Onuki and R. A. Ferrell, Physica A **164**, 245 (1990).

[6] R. P. Behringer, A. Onuki, and H. Meyer, J. Low Temp. Phys. **81**, 71 (1990).

[7] C. E. Pittman, L. H. Cohen, and H. Meyer, J. Low Temp. Phys. **46**, 115 (1982).

[8] L. H. Cohen, M. L. Dingus, and H. Meyer, J. Low Temp. Phys. **61**, 79 (1985).

[9] J. Straub, doctoral thesis, Technical University, Munich, 1965 (unpublished).

[10] L. Eicher, Semesterarbeit, Technical University, Munich, 1991 (unpublished).

[11] R. A. Wilkinson, R. F. Berg, R. W. Gammon, L. Eicher, M. R. Moldover, and J. Straub (unpublished).

[12] F. Zhong and H. Meyer, Bull. Am. Phys. Soc. **38**, 1006 (1993).

[13] R. A. Ferrell and A. Onuki (unpublished).

[14] L. D. Landau and E. M. Lifshitz, *Fluid Mechanics* (Pergamon, New York, 1959), Sec. 49.

[15] H. Hao (private communication).

[16] M. R. Moldover, J. V. Sengers, R. W. Gammon, and R. J. Hocken, Rev. Mod. Phys. **51**, 79 (1979).

[17] H. E. Stanley, *Introduction to Phase Transitions and Critical Point Phenomena* (Oxford University Press, New York, 1971).